

Ultrafast demagnetization after laser irradiation in transition metals: *Ab initio* calculations of the spin-flip electron-phonon scattering with reduced exchange splitting

Christian Illg, Michael Haag, and Manfred Fähnle*

Max Planck Institute for Intelligent Systems, Heisenbergstr. 3, 70569 Stuttgart, Germany

(Received 23 September 2013; revised manuscript received 15 November 2013; published 6 December 2013)

Despite intensive research, the underlying mechanisms for ultrafast demagnetization after laser irradiation in transition metals are still not understood. We discuss the possible processes which have been suggested in order to explain the ultrafast demagnetization within several hundreds of femtoseconds and argue that the spin angular momentum has to go to the lattice in the end. Based on this argument, we consider spin-flip electron-phonon scatterings. The demagnetization time τ_M and the demagnetization rate dM/dt due to spin-flip electron-phonon scattering is calculated for fcc Ni and bcc Fe. Thereby, the electronic states and phononic states are calculated *ab initio*. We find that the demagnetization rates for fcc Ni and bcc Fe are too small to explain experimental demagnetization rates, which is in agreement with earlier publications. In addition, the demagnetization rates for band structures with reduced exchange splitting are calculated, however, also these demagnetization rates are too small. Finally, the phase space for scattering processes which is related to the maximum possible demagnetization is estimated for band structures with ground-state exchange splitting and with reduced exchange splitting. The maximum possible demagnetization is too small for bcc Fe and fcc Co but not necessarily for fcc Ni. We suggest to include magnons and to consider independent combinations of spin-flip electron-phonon and spin-flip electron-magnon scattering processes as a possible explanation for the ultrafast demagnetization.

DOI: [10.1103/PhysRevB.88.214404](https://doi.org/10.1103/PhysRevB.88.214404)

PACS number(s): 71.70.Ej, 75.70.Tj, 75.78.Jp, 78.47.J-

I. INTRODUCTION

In 1996, Beaupaire *et al.*¹ showed for the first time that a thin ferromagnetic Ni film demagnetizes within several hundreds of femtoseconds (fs) after irradiation with a short (60 fs) linearly polarized laser pulse. This was a real milestone in the research of magnetization dynamics because of the unprecedented very short time scale. Thereafter, a lot of effort was made to investigate this so-called “ultrafast demagnetization” both experimentally and theoretically. The experimental results of Beaupaire *et al.* were confirmed in many other publications (for a review, see, e.g., Ref. 2). Further experiments for Fe (Ref. 3) and for Co (Ref. 4) demonstrated an ultrafast demagnetization on the same time scale (several hundreds of fs). A lot of theoretical suggestions have been made to explain the ultrafast demagnetization in Ni, Fe, and Co, however, until now the underlying mechanisms are not understood. The suggestions are discussed in the following.

The expectation value $\langle S_e \rangle$ of the electronic spin momentum related to the spin angular momentum operator \hat{S}_e and the expectation value $\langle L_e \rangle$ of the orbital angular momentum related to the orbital momentum operator \hat{L}_e of the electrons build the magnetization \mathbf{M} :

$$\mathbf{M} \propto \langle L_e \rangle + g \langle S_e \rangle, \quad (1)$$

where $g \approx 2$ is the spin g factor. The expectation value $\langle L_e \rangle$ of the orbital angular momentum is usually nearly completely quenched in crystals of transition metals which are considered in this paper (this does not hold for all ferromagnets, e.g., for rare-earth metals). Hence, the magnetization is built by the expectation value $\langle S_e \rangle$ of the spin angular momentum in a good approximation. When the magnetization \mathbf{M} decreases during the ultrafast demagnetization, also the expectation value $\langle S_e \rangle$ of the spin angular momentum has to decrease.

If angular momentum conservation holds, the fundamental question is as follows: Where does angular momentum related to the expectation value $\langle S_e \rangle$ go to? In Ref. 5, it is discussed extensively that the conditions for angular momentum conservation are approximately fulfilled during the ultrafast demagnetization experiment. The angular momentum conservation reads as⁵⁻⁸

$$\Delta \langle \mathbf{J} \rangle = \Delta \langle \mathbf{L}_e \rangle + \Delta \langle \mathbf{S}_e \rangle + \Delta \langle \mathbf{L}_l \rangle + \Delta \langle \mathbf{L}_{ph} \rangle = 0, \quad (2)$$

where Δ denotes the difference and $\langle \mathbf{J} \rangle$, $\langle \mathbf{L}_l \rangle$, and $\langle \mathbf{L}_{ph} \rangle$ are the expectation value of the total angular momentum, the expectation value of the angular momentum of the lattice, and the expectation value of the angular momentum of the laser photons, respectively. In the following, several possibilities for underlying mechanisms for ultrafast demagnetization are discussed:

(1) *Interaction with laser photons.* Several authors⁹⁻¹² suggested that the direct interaction with the laser photons could be the reason for the ultrafast demagnetization due to angular momentum transfer from $\langle \mathbf{L}_{ph} \rangle$ to $\langle \mathbf{S}_e \rangle$. However, estimations showed⁶ that the photoquenching is only $10^{-4} \mu_B$ per atom in Ni which is too small to explain the ultrafast demagnetization (Ni has a ground-state magnetic moment of $0.64 \mu_B$ per atom). Also, recent experiments^{7,13} could not prove a noticeable demagnetization effect by laser photons alone.

(2) *Emission of photons.* Emission of photons during ultrafast demagnetization was measured^{14,15} and it was found that the emitted light is linearly polarized and in the THz frequency range. As shown in Ref. 16, for a spherically symmetric system the integral of the electromagnetic angular momentum density of an electromagnetic wave taken over the whole volume vanishes. For the geometries used in the demagnetization experiments, however, the situation is not spherically symmetric. It could also be that the emitted photons

are reabsorbed again,⁵ and in a dichroic material this leads to a preference of the direction of electron-photon spin-flip processes, for instance, there may be more scattering processes from spin up to spin down⁶ and this may contribute to the demagnetization.⁵ Nevertheless, it is generally believed that the demagnetization effect of emitted photons is rather small.

(3) *Electron-phonon interaction.* An often discussed explanation for ultrafast demagnetization is the spin-flip electron-phonon scattering via the Elliott-Yafet mechanism^{17,18} which leads to an angular momentum transfer from $\langle S_e \rangle$ to $\langle L_l \rangle$. *Ab initio* calculations for the demagnetization effect due to spin-flip electron-phonon scattering were done for fcc Ni, bcc Fe, and fcc Co,^{19–22} however, the demagnetization due to spin-flip electron-phonon scattering was always too small to explain the experimental demagnetization. It was claimed in Ref. 20 that calculations with a rigid-band structure could never explain experimental demagnetization rates and that a calculation which takes into account the modification of the exchange splitting (and hence a modification of the band structure) arising from a change of the magnetization in time due to demagnetization could possibly reproduce experimental demagnetization rates. All calculations with electron-phonon scattering (also the calculations in this paper) have in common that linearly polarized phonon states are used which do not have a well-defined angular momentum and the expectation value of the angular momentum is zero,^{2,23} i.e., one does not keep track of the angular momentum conservation in the single electron-phonon-scattering process and assumes implicitly that the lattice is a perfect sink for the angular momentum. In principle, it is possible to use circularly or elliptically polarized phonon states which have a well-defined angular momentum²³ (but which are not stationary) to keep track of the angular momentum conservation.

(4) *Electron-electron interaction.* Electron-electron scattering is definitely very important since Coulomb interaction is dominant and electron-electron scattering is a very fast process.⁴ Without spin-orbit coupling, it is not possible to change the expectation value $\langle S_e \rangle$ of the spin angular momentum by these scatterings. With spin-orbit coupling, it is possible to change $\langle S_e \rangle$, for example, via an angular momentum flow from $\langle S_e \rangle$ to $\langle L_e \rangle$. Stamm *et al.*^{24,25} and Boeglin *et al.*²⁶ showed with x-ray magnetic circular dichroism (XMCD) experiments that both $\langle S_e \rangle$ and $\langle L_e \rangle$ decrease during the ultrafast demagnetization. Therefore, an increase of $\langle L_e \rangle$ could only be possible within a time scale faster than the temporal resolution of Refs. 24–26. Krauss *et al.*²⁷ made model calculations with electron-electron scattering in systems with spin-orbit coupling and came to the conclusion that electron-electron scattering could be the reason for ultrafast demagnetization. Thereby, it is assumed that the electronic angular momentum is very quickly transferred to the lattice $\langle L_l \rangle$. Mueller *et al.*²⁸ also made model calculations which included both electron-electron and electron-phonon scattering. They found out that the electron-electron scattering is essential for the demagnetization (whereas the phonon cooling is essential for the remagnetization). Thereby, it is also assumed that the electronic angular momentum is very quickly transferred to the lattice $\langle L_l \rangle$ (they also do not keep track of angular momentum conservation).

(5) *Electron-magnon interaction.* In a system without spin-orbit coupling it is not possible to change the spin angular momentum $\langle S_e \rangle$ via electron-magnon scattering. In a system with spin-orbit coupling it is possible to reduce $\langle S_e \rangle$ via electron-magnon scattering. It was suggested in Ref. 3 that angular momentum is transferred from $\langle S_e \rangle$ to $\langle L_e \rangle$ via electron-magnon scattering and subsequently $\langle L_e \rangle$ is quenched by the crystal field. If this mechanism is relevant, the crystal field quenching has to be faster than the temporal resolution of Refs. 24–26.

(6) *Electron-defect and electron-interface scattering.* Demagnetization experiments were done for different samples,²⁹ namely, epitaxial thin films, polycrystalline films, and surfaces of single crystals. The results for the demagnetization time were always similar [about 200 fs (Ref. 29)] and it must be concluded that the demagnetization time is an intrinsic property which is nearly independent from electron-defect and electron-interface scattering.

(7) *Phonon-phonon interaction.* In the Einstein–de Haas effect,³⁰ the sudden change of the magnetization of a paramagnetic cylinder is compensated by a rotation of the cylinder due to angular momentum conservation. The same effect was discussed⁶ in the context of the ultrafast demagnetization experiment by raising the question as to whether the reduction of $\langle S_e \rangle$ could result in a net rotation of the irradiated area of the sample. A net rotation is a $\mathbf{q} = 0$ mode where \mathbf{q} is the phonon wave vector. In order to end up in a $\mathbf{q} = 0$ mode, phonon-phonon interaction via anharmonicities is necessary. It is argued in Ref. 5 that phonon-phonon interaction is too slow for a 100-fs time scale and, therefore, the mechanism of the Einstein–de Haas effect is not the reason for ultrafast demagnetization, as also assumed in Ref. 6.

(8) *Phonon-magnon interaction.* Scattering processes of phonons with magnons are much slower (on a 100-ps time scale³¹) than electron-phonon scattering processes (on a 20-fs time scale, see Sec. IV) and it is generally believed that phonon-magnon scattering is too slow for an ultrafast demagnetization dynamics in fcc Ni and fcc Co,⁴ but possibly it is relevant for the demagnetization in Gd (Refs. 32 and 33) and Tb.³³

(9) *Superdiffusive spin transport.* It was shown by Battiato *et al.*^{34,35} that a demagnetization can also be explained without any spin-flip channel but with a superdiffusive spin transport where the majority electrons diffuse faster into the substrate than the minority electrons. Very recent measurements^{13,36–38} support the notion that this mechanism can contribute to the demagnetization, but it was also shown that this contribution depends critically on the composition of the system³⁹ and that it is not the dominant effect in simple ferromagnetic films on an insulating substrate.⁴⁰

Altogether, it must be concluded that the angular momentum has to go from the spin degrees of freedom to the lattice, and in most publications it is assumed implicitly or explicitly that the spin angular momentum $\langle S_e \rangle$ flows to the lattice $\langle L_l \rangle$ in the end. Therefore, we investigate electron-phonon scattering in the following. It might be that there are other processes, e.g., electron-electron scattering processes which are faster, however, in this case the electron-phonon scattering is certainly the “bottleneck” since finally the angular momentum has to go to the lattice.

In this paper, the spin-flip electron-phonon scattering is investigated by *ab initio* calculations, i.e., we also assume that the angular momentum is transferred from $\langle \mathbf{S}_e \rangle$ to $\langle \mathbf{L}_l \rangle$ but we do not keep track of the angular momentum conservation and consider the lattice as a perfect sink for angular momentum. Similar calculations were published by Essert and Schneider^{20,21} and Carva *et al.*^{19,22} In contrast to Refs. 20 and 21, we do not calculate the occupation distribution of electronic states directly after the laser pulse irradiation, but it is our main assumption that the electrons thermalize very quickly via electron-electron scattering and that the thermalized electrons are responsible for the demagnetization. This is in line with an earlier publication.⁴ In contrast to Refs. 19 and 22, we do not make supercell calculations but we use the rigid-ion approximation for the scattering operator⁴¹ which in principle allows us to calculate the scattering matrix element for any phonon wave vector \mathbf{q} (in Ref. 22, a comparison of the supercell calculations with calculations in rigid-ion approximation is made and they agree quite well). Furthermore, we go beyond the four above-mentioned publications because we calculate the demagnetization rates and the available phase space for scattering (which is linked to the maximum possible demagnetization) also for band structures with reduced magnetic moment, i.e., reduced exchange splitting.

This paper is organized as follows: In Sec. II, the electron-phonon-scattering matrix element in rigid-ion approximation, Fermi's golden rule, and the Boltzmann rate equations are presented which are used for the equations for the demagnetization time τ_M and for the demagnetization rate dM/dt . The implementation with the linear-muffin-tin-orbital method is explained in Sec. III. In Sec. IV, the results for a ground-state exchange splitting and for exchange splittings according to reduced magnetic moments are shown. The phase-space estimation which is linked to the maximum possible demagnetization is explained in Sec. V and results are shown. Finally, the results are discussed and conclusions are drawn in Sec. VI.

II. FORMALISM

A. Fermi's golden rule

In a system with spin-orbit coupling, the electronic states are always spin mixed,

$$\Psi_{j\mathbf{k}} = [a_{j\mathbf{k}}(\mathbf{r})|\chi_\uparrow\rangle + b_{j\mathbf{k}}(\mathbf{r})|\chi_\downarrow\rangle] \cdot \exp(i\mathbf{k}\mathbf{r}), \quad (3)$$

where $a_{j\mathbf{k}}(\mathbf{r})$ and $b_{j\mathbf{k}}(\mathbf{r})$ are lattice-periodic functions (j denotes the band index, \mathbf{k} is the wave vector) and $|\chi_\uparrow\rangle$ and $|\chi_\downarrow\rangle$ are the two spinor eigenfunctions. Thereby, the wave function is denoted as "dominant spin up" or "dominant spin down" if $p_{j\mathbf{k}}^\uparrow = \langle \Psi_{j\mathbf{k}} | \chi_\uparrow \rangle \langle \chi_\uparrow | \Psi_{j\mathbf{k}} \rangle$ is larger than or less than $p_{j\mathbf{k}}^\downarrow = \langle \Psi_{j\mathbf{k}} | \chi_\downarrow \rangle \langle \chi_\downarrow | \Psi_{j\mathbf{k}} \rangle$. In the following, we denote the dominant spin character by $s = \uparrow, \downarrow$.

The transition rate $W_{j\mathbf{k}s, j'\mathbf{k}'s'}$ for a transition from a state $\Psi_{j\mathbf{k}}^s$ with energy $\varepsilon_{j\mathbf{k}}^s$ to a state $\Psi_{j'\mathbf{k}'}^{s'}$ with energy $\varepsilon_{j'\mathbf{k}'}^{s'}$ (j, j' denote the band indices, \mathbf{k}, \mathbf{k}' are the wave vectors, and s, s' denote the dominant spin character) via spin-flip scattering of electrons at linearly polarized phonons is given in Fermi's

golden rule:¹⁸

$$W_{j\mathbf{k}s, j'\mathbf{k}'s'}^\lambda = \frac{2\pi}{\hbar} |M_{j\mathbf{k}s, j'\mathbf{k}'s'}^\lambda|^2 \frac{\hbar}{2N M \omega_{\mathbf{q}\lambda}} \times \{ b_{\mathbf{q}\lambda} \delta[\varepsilon_{j'\mathbf{k}'}^{s'} - (\varepsilon_{j\mathbf{k}}^s + \hbar\omega_{\mathbf{q}\lambda})] + (b_{-\mathbf{q}\lambda} + 1) \delta[\varepsilon_{j'\mathbf{k}'}^{s'} - (\varepsilon_{j\mathbf{k}}^s - \hbar\omega_{-\mathbf{q}\lambda})] \}. \quad (4)$$

The phonon with wave vector \mathbf{q} has frequencies $\omega_{\mathbf{q}\lambda}$ and polarization vectors $\mathbf{n}_{\mathbf{q}\lambda}$ where λ denotes the three polarizations. Thereby, momentum conservation is demanded $\mathbf{k} + \mathbf{q} = \mathbf{k}' + \mathbf{G}$ where \mathbf{G} is a reciprocal lattice vector. $b_{\mathbf{q}\lambda} = [\exp(\hbar\omega_{\mathbf{q}\lambda}/k_B T_p) - 1]^{-1}$ is the Bose distribution function where k_B is Boltzmann's constant and T_p is the phonon temperature. N is the number of atoms and M is the atomic mass. Absorption of phonons and both induced and spontaneous emission of phonons are included in Eq. (4). $M_{j\mathbf{k}s, j'\mathbf{k}'s'}^\lambda$ is the transition matrix element which reads as

$$M_{j\mathbf{k}s, j'\mathbf{k}'s'}^\lambda = \langle \Psi_{j'\mathbf{k}'}^{s'} | W_{\mathbf{q}\lambda} | \Psi_{j\mathbf{k}}^s \rangle \quad (5)$$

and $W_{\mathbf{q}\lambda}$ is defined by¹⁸

$$W_{\mathbf{q}\lambda} = \sum_{n=1}^N \exp(i\mathbf{q}\mathbf{R}_{0,n}) (\mathbf{n}_{\mathbf{q}\lambda} \cdot \nabla_{\mathbf{R}_n}) \times \left[\begin{pmatrix} V^\uparrow(\mathbf{r}; \{\mathbf{R}_n\}) & 0 \\ 0 & V^\downarrow(\mathbf{r}; \{\mathbf{R}_n\}) \end{pmatrix} + \sum_i \frac{\hbar}{4m_e^2 c^2} (\nabla_{\mathbf{r}} V^\alpha(\mathbf{r}; \{\mathbf{R}_n\}) \times \hat{\mathbf{p}})_i \hat{\sigma}_i \right] \Big|_{\mathbf{R}_n = \mathbf{R}_{0,n}}, \quad (6)$$

which includes a distortion of the lattice potential (first term, Elliott part) and a distortion of the spin-orbit coupling (second term, Yafet part). $V^\alpha(\mathbf{r}; \{\mathbf{R}_n\})$ denotes the effective potential of the spin-density-functional theory that an electron at position \mathbf{r} feels ($\alpha = \uparrow, \downarrow$). This potential depends on the set of positions of lattice atoms $\{\mathbf{R}_n\}$. The position of the n th lattice atom \mathbf{R}_n is given by $\mathbf{R}_n = \mathbf{R}_{0,n} + \delta\mathbf{R}_n$ where $\mathbf{R}_{0,n}$ is the equilibrium position and $\delta\mathbf{R}_n$ is the displacement. m_e and c denote the electron mass and the speed of light, respectively. $\hat{\mathbf{p}}$ is the momentum operator and $\hat{\sigma}_i$ the i th Pauli matrix.

It is possible to subdivide the equilibrium potential $V_0^\alpha(\mathbf{r}; \{\mathbf{R}_{0,n}\})$ into equilibrium atomic potentials $v_{0,n}^\alpha(\mathbf{r} - \mathbf{R}_{0,n})$ (defined in an atomic sphere and zero outside) around the equilibrium position of the lattice atoms $\mathbf{R}_{0,n}$:

$$V_0^\alpha(\mathbf{r}; \{\mathbf{R}_{0,n}\}) = \sum_{n=1}^N v_{0,n}^\alpha(\mathbf{r} - \mathbf{R}_{0,n}). \quad (7)$$

In the rigid-ion approximation,⁴¹ it is assumed that the atomic potentials are displaced rigidly without deformation:

$$V^\alpha(\mathbf{r}; \{\mathbf{R}_n\}) \approx \sum_{n=1}^N v_{0,n}^\alpha(\mathbf{r} - \mathbf{R}_n). \quad (8)$$

This is a good approximation for transition metals,^{22,42} at least for not too small \mathbf{q} . However, the rigid-ion approximation neglects the screening of the electron-phonon interaction which modifies the matrix element for $\mathbf{q} \rightarrow 0$ (see Refs. 43 and 44). It is straightforward to show that $W_{\mathbf{q}\lambda}$ in the rigid-ion

approximation reads as

$$W_{\mathbf{q}\lambda} = \sum_{n=1}^N -\exp(i\mathbf{q}\mathbf{R}_{0,n}) (\mathbf{n}_{\mathbf{q}\lambda} \cdot \nabla_{\mathbf{r}}) \times \left[\begin{pmatrix} v_{0,n}^{\uparrow}(\mathbf{r} - \mathbf{R}_{0,n}) & 0 \\ 0 & v_{0,n}^{\downarrow}(\mathbf{r} - \mathbf{R}_{0,n}) \end{pmatrix} + \sum_i \frac{\hbar}{4m_e^2 c^2} [\nabla_{\mathbf{r}} v_{0,n}^{\alpha}(\mathbf{r} - \mathbf{R}_{0,n}) \times \hat{\mathbf{p}}]_i \hat{\sigma}_i \right]. \quad (9)$$

Local coordinates can be defined: $\mathbf{r}_n \equiv \mathbf{r} - \mathbf{R}_{0,n}$. If the atomic potentials are spherically symmetric $v_{0,n}^{\alpha}(\mathbf{r}_n) = v_{0,n}^{\alpha}(r_n)$, Eq. (9) can be rewritten as

$$W_{\mathbf{q}\lambda} = \sum_{n=1}^N -\exp(i\mathbf{q}\mathbf{R}_{0,n}) (\mathbf{n}_{\mathbf{q}\lambda} \cdot \nabla_{\mathbf{r}_n}) \left[\begin{pmatrix} v_{0,n}^{\uparrow}(r_n) & 0 \\ 0 & v_{0,n}^{\downarrow}(r_n) \end{pmatrix} + \sum_i \frac{\hbar}{4m_e^2 c^2 r_n} \frac{\partial v_{0,n}^{\alpha}}{\partial r_n} (\hat{\mathbf{L}}_n)_i \hat{\sigma}_i \right], \quad (10)$$

where $\hat{\mathbf{L}}_n = \mathbf{r}_n \times \hat{\mathbf{p}}$ is the angular momentum operator.

B. Discussion of Fermi's golden rule

Fermi's golden rule is derived in a time-dependent perturbation theory of first order. The higher orders are small if the perturbation time t_p is short and if the perturbation strength is weak. However, in order to replace the $\sin x/x$ function (appearing in the derivation of Fermi's golden rule) by the δ distribution, it is assumed that the perturbation time t_p is long enough. A rough criterion is that the full width at half maximum $2\pi\hbar/t_p$ of the $\sin x/x$ function is much smaller than the maximum energy width $\Delta\varepsilon$ between the final and the initial states

$$\frac{2\pi\hbar}{t_p} \ll \Delta\varepsilon. \quad (11)$$

The maximum energy width between initial and final states is about 40 meV for electron-phonon scattering. Therefore, the perturbation time has to fulfill the criterion $t_p \gg 100$ fs. Furthermore, Fermi's golden rule has a Markov character, i.e., the processes do not depend on preceding processes which also does not hold on a fs time scale. Therefore, the use of Fermi's golden rule is in principle not allowed on a fs time scale, instead quantum-kinetic calculations are necessary. However, there is a publication⁴⁵ which shows for laser-irradiated semiconductors that the difference between a quantum-kinetic calculation and a calculation with Boltzmann rate equations (which are Markovian) using Fermi's golden rule is small for averaged quantities already after some fs, whereas the results for spectrally resolved quantities are different. Hence, it is reasonable to assume that our main quantities, the demagnetization time τ_M and the demagnetization rate dM/dt , which are related to the electronic spin moments

averaged over all electronic energies, are correct despite using Fermi's golden rule and Boltzmann rate equations.

C. Demagnetization rate

Within Boltzmann's theory, the time-dependent total transition rate $W^{s,s'}(t)$ from spin character s to spin character s' reads as^{18,46}

$$W^{s,s'}(t) = \frac{1}{\Omega_{\text{BZ}}^2} \sum_{j,j',\lambda} \int_{\text{BZ}} d^3k \int_{\text{BZ}} d^3k' f_i(\varepsilon_{j\mathbf{k}}^s) [1 - f_i(\varepsilon_{j'\mathbf{k}'}^{s'})] \times W_{j\mathbf{k}s,j'\mathbf{k}'s'}^{\lambda}, \quad (12)$$

where Ω_{BZ} is the Brillouin zone (BZ) volume and f_i is the time-dependent Fermi distribution function

$$f_i(\varepsilon_{j\mathbf{k}}^s) \equiv \left[\exp\left(\frac{\varepsilon_{j\mathbf{k}}^s - \varepsilon_{\text{F}}^s(t)}{k_{\text{B}} T_e(t)}\right) + 1 \right]^{-1} \quad (13)$$

with the time-dependent chemical potential $\varepsilon_{\text{F}}^s(t)$ and the time-dependent electron temperature $T_e(t)$.

The demagnetization rate dM/dt (more precisely, rate of the magnetic moment change per atom) is given by

$$\frac{dM}{dt} = \frac{1}{\Omega_{\text{BZ}}^2} \sum_{j,j',\lambda} \int_{\text{BZ}} d^3k \int_{\text{BZ}} d^3k' m_{j\mathbf{k}\uparrow,j'\mathbf{k}'\downarrow} \times \{ f_i(\varepsilon_{j\mathbf{k}}^{\uparrow}) [1 - f_i(\varepsilon_{j'\mathbf{k}'}^{\downarrow})] W_{j\mathbf{k}\uparrow,j'\mathbf{k}'\downarrow}^{\lambda} - f_i(\varepsilon_{j'\mathbf{k}'}^{\downarrow}) [1 - f_i(\varepsilon_{j\mathbf{k}}^{\uparrow})] W_{j'\mathbf{k}'\downarrow,j\mathbf{k}\uparrow}^{\lambda} \}. \quad (14)$$

$m_{j\mathbf{k}\uparrow,j'\mathbf{k}'\downarrow}$ keeps track of the spin magnetic moment change for every spin-flip transition. For pure spin states, $m_{j\mathbf{k}\uparrow,j'\mathbf{k}'\downarrow}$ equals $2\mu_{\text{B}}$ but for spin-mixed states (in systems with spin-orbit coupling) it is less than $2\mu_{\text{B}}$.

D. Demagnetization time

Yafet considered a situation in which a paramagnet is in a magnetic field and at some time the magnetic field is switched off. Thereafter, the paramagnet relaxes to its equilibrium and a relaxation time can be defined.¹⁸

The ultrafast demagnetization experiment is totally different, but nevertheless it was shown that a demagnetization time τ_M can be defined⁴⁶ for ferromagnets in analogy to Yafet's definition of the relaxation time if the following conditions hold:

- (1) Most states have an almost pure spin character, i.e., the spin mixing is rather small.
- (2) The system is near the equilibrium situation.
- (3) The decrease of magnetization is exponential.

The first condition is approximately fulfilled for transition metals.^{47,48} The second condition is fulfilled if only thermalized electrons contribute to the demagnetization (in accordance with Ref. 4) and in addition if the electron temperature is near 300 K. The third condition is in accordance with the measurements.⁴

According to Ref. 46, the demagnetization time reads as

$$\frac{1}{\tau_M} = \frac{1}{\Omega_{\text{BZ}}^2} \sum_{j,j',\lambda} \int_{\text{BZ}} d^3k \int_{\text{BZ}} d^3k' \left\{ W_{j\mathbf{k}\uparrow,j'\mathbf{k}'\downarrow}^{\lambda} \left[\frac{f_0(\varepsilon_{j\mathbf{k}}^{\uparrow}) \eta(\varepsilon_{j'\mathbf{k}'}^{\downarrow})}{\tilde{Z}^{\downarrow}(\varepsilon_{\text{F}}^0)} + \frac{[1 - f_0(\varepsilon_{j'\mathbf{k}'}^{\downarrow})] \eta(\varepsilon_{j\mathbf{k}}^{\uparrow})}{\tilde{Z}^{\uparrow}(\varepsilon_{\text{F}}^0)} \right] + W_{j'\mathbf{k}'\downarrow,j\mathbf{k}\uparrow}^{\lambda} \left[\frac{f_0(\varepsilon_{j'\mathbf{k}'}^{\downarrow}) \eta(\varepsilon_{j\mathbf{k}}^{\uparrow})}{\tilde{Z}^{\uparrow}(\varepsilon_{\text{F}}^0)} + \frac{[1 - f_0(\varepsilon_{j\mathbf{k}}^{\uparrow})] \eta(\varepsilon_{j'\mathbf{k}'}^{\downarrow})}{\tilde{Z}^{\downarrow}(\varepsilon_{\text{F}}^0)} \right] \right\}. \quad (15)$$

The Fermi distribution function in equilibrium is

$$f_0(\varepsilon) \equiv \left[\exp\left(\frac{\varepsilon - \varepsilon_F^0}{k_B T_0}\right) + 1 \right]^{-1}, \quad (16)$$

where ε_F^0 is the equilibrium chemical potential and T_0 is the equilibrium temperature. $\eta(\varepsilon)$ is the derivative of the Fermi distribution function

$$\eta(\varepsilon) \equiv -\frac{\partial f_0(\varepsilon)}{\partial \varepsilon} \quad (17)$$

and $\tilde{Z}^s(\varepsilon_F^0)$ is defined by

$$\tilde{Z}^s(\varepsilon_F^0) \equiv \int_{-\infty}^{+\infty} d\varepsilon Z^s(\varepsilon) \eta(\varepsilon), \quad (18)$$

where $Z^s(\varepsilon)$ is the spin-resolved density of states.

The main difference between the demagnetization time τ_M and the demagnetization rate dM/dt is that only equilibrium quantities enter Eq. (15) for the demagnetization time and that nonequilibrium quantities enter Eq. (14) for the demagnetization rate. The nonequilibrium quantities are the chemical potentials $\varepsilon_F^s(t)$ and the electron temperature $T_e(t)$.

III. AB INITIO METHODS AND IMPLEMENTATION

The electronic states are calculated *ab initio* with the relativistic version⁴⁹ of the linear-muffin-tin-orbital (LMTO) method⁵⁰ in local-spin-density approximation^{51,52} (LSDA) and in atomic-sphere approximation (ASA).⁵⁰ The crystal wave functions are expanded in atomic functions $\Phi_{\mathbf{R}_{0,n}lm\alpha}$ and their energy derivatives $\dot{\Phi}_{\mathbf{R}_{0,n}lm\alpha}$ (l, m, α are the angular momentum quantum number, the magnetic quantum number, and the spin quantum number, respectively):

$$\begin{aligned} \Psi_{j\mathbf{k}}^s(\mathbf{r}) &= \sqrt{\frac{1}{N}} \sum_{n=1}^N \exp(i\mathbf{k}\mathbf{R}_{0,n}) \\ &\times \left[\sum_{lm\alpha} c_{lm\alpha}^{j\mathbf{k}s} \Phi_{\mathbf{R}_{0,n}lm\alpha}(\mathbf{r}) + d_{lm\alpha}^{j\mathbf{k}s} \dot{\Phi}_{\mathbf{R}_{0,n}lm\alpha}(\mathbf{r}) \right], \end{aligned} \quad (19)$$

where $c_{lm\alpha}^{j\mathbf{k}s}$ and $d_{lm\alpha}^{j\mathbf{k}s}$ are the expansion coefficients. The crystal wave function $\Psi_{j\mathbf{k}}^s$, the atomic function $\Phi_{\mathbf{R}_{0,n}lm\alpha}$, and its energy derivative $\dot{\Phi}_{\mathbf{R}_{0,n}lm\alpha}$ are four-vectors with large component and small component.⁴⁹

The matrix elements in Eq. (5) have a simple form in ASA:

$$\begin{aligned} M_{j\mathbf{k}s, j'\mathbf{k}'s'}^\lambda &= \frac{1}{N} \sum_{n, n'=1}^N \exp[i(\mathbf{k}\mathbf{R}_{0,n} - \mathbf{k}'\mathbf{R}_{0,n'})] \\ &\times \sum_{\substack{lm\alpha \\ l'm'\alpha'}} \left\{ (c_{l'm'\alpha'}^{j'\mathbf{k}'s'})^* c_{lm\alpha}^{j\mathbf{k}s} \langle \Phi_{\mathbf{R}_{0,n'}l'm'\alpha'} | W_{\mathbf{q}\lambda} | \Phi_{\mathbf{R}_{0,n}lm\alpha} \rangle \right. \\ &+ (c_{l'm'\alpha'}^{j'\mathbf{k}'s'})^* d_{lm\alpha}^{j\mathbf{k}s} \langle \Phi_{\mathbf{R}_{0,n'}l'm'\alpha'} | W_{\mathbf{q}\lambda} | \dot{\Phi}_{\mathbf{R}_{0,n}lm\alpha} \rangle \\ &+ (d_{l'm'\alpha'}^{j'\mathbf{k}'s'})^* c_{lm\alpha}^{j\mathbf{k}s} \langle \dot{\Phi}_{\mathbf{R}_{0,n'}l'm'\alpha'} | W_{\mathbf{q}\lambda} | \Phi_{\mathbf{R}_{0,n}lm\alpha} \rangle \\ &\left. + (d_{l'm'\alpha'}^{j'\mathbf{k}'s'})^* d_{lm\alpha}^{j\mathbf{k}s} \langle \dot{\Phi}_{\mathbf{R}_{0,n'}l'm'\alpha'} | W_{\mathbf{q}\lambda} | \dot{\Phi}_{\mathbf{R}_{0,n}lm\alpha} \rangle \right\} \end{aligned} \quad (20)$$

and momentum conservation $\mathbf{k} + \mathbf{q} = \mathbf{k}' + \mathbf{G}$ automatically arises when Eq. (20) is evaluated. The potential $v_{0,n}^\alpha(r_n)$ and the spin-orbit coupling $\sum_i \hbar/(4m_e^2 c^2 r_n) \partial v_{0,n}^\alpha / \partial r_n (\hat{\mathbf{L}}_n)_i \hat{\sigma}_i$ included in $W_{\mathbf{q}\lambda}$ has to be replaced by the corresponding relativistic LMTO expressions.⁴⁹ We calculate the matrix element $M_{j\mathbf{k}s, j'\mathbf{k}'s'}^\lambda$ including the large and small components without any approximation.

The phonon frequencies $\omega_{\mathbf{q}\lambda}$ and polarization vectors $\mathbf{n}_{\mathbf{q}\lambda}$ are obtained from a force-constant model.⁵³ Thereby, the force constants are calculated *ab initio* with the pseudopotential method using QUANTUM ESPRESSO,⁵⁴ Vanderbilt ultrasoft pseudopotentials,⁵⁵ and the generalized gradient approximation.⁵⁶ All *ab initio* quantities are calculated for zero temperature and it is assumed that they are still correct for higher temperatures.

The nonequilibrium quantities $\varepsilon_F^s(t)$ and $T_e(t)$ can not be calculated *ab initio*. The electron temperature $T_e(t)$ is considered as a parameter and one can obtain reasonable values from experimental publications^{1,4,57,58} which are between 400 and 1000 K. The chemical potentials $\varepsilon_F^{\uparrow, \downarrow}$ can be determined with two conditions for the time t_s where the thermalization via electron-electron scattering is finished. As already explained above, it is our main assumption that thermalized electrons make the main contribution to the demagnetization, in accordance with Ref. 4. Therefore, at time t_s , the magnetization is still the equilibrium magnetization M_0 (first condition). Without superdiffusive spin transport, number conservation holds for any time t , $N_0 = N^\uparrow(t) + N^\downarrow(t)$, where N_0 is the total number of valence electrons in equilibrium and $N^{\uparrow, \downarrow}$ is the number of spin-up and -down electrons, respectively,

$$N^{\uparrow, \downarrow}(t) = \int_{-\infty}^{+\infty} d\varepsilon Z^{\uparrow, \downarrow}(\varepsilon) f_t(\varepsilon^{\uparrow, \downarrow}). \quad (21)$$

The number conservation holds especially for time t_s (second condition). Both conditions

$$N_0 = N^\uparrow(t_s) + N^\downarrow(t_s), \quad M_0 = \mu_B [N^\uparrow(t_s) - N^\downarrow(t_s)] \quad (22)$$

enable the determination of the chemical potentials $\varepsilon_F^{\uparrow, \downarrow}(t_s)$.

We also want to calculate the demagnetization rate for times t_* ($t_* > t_s$) where the magnetization has already reduced to $M_* = M(t_*)$ and M_* is considered as a given parameter. The two conditions in order to calculate $\varepsilon_F^{\uparrow, \downarrow}(t_*)$ read as

$$N_0 = N^\uparrow(t_*) + N^\downarrow(t_*), \quad M_* = \mu_B [N^\uparrow(t_*) - N^\downarrow(t_*)]. \quad (23)$$

In order to evaluate the δ function on a discrete k -point grid it is necessary to smear the δ function. The δ function is represented by its Gaussian identity with the smearing parameter σ :

$$\delta_\sigma(\varepsilon) \equiv \frac{1}{\sqrt{\pi\sigma^2}} \exp\left(-\frac{\varepsilon^2}{\sigma^2}\right). \quad (24)$$

Different smearing parameters σ have to be tested.

One can show that only states with energies which are not too far away from the Fermi energy are relevant for the calculation of the demagnetization time and the demagnetization rate. We use this fact and choose the relevant energy range around the Fermi energy appropriately.

IV. RESULTS

The calculations are made for different k -point grids and for different smearing parameters σ . We checked carefully for convergence keeping the product $\sigma \cdot N_1$ constant (N_1 is the number of k points in one direction). The largest k -point grid which we considered has $50 \times 50 \times 50$ k points in the first Brillouin zone. It turns out that the convergence is very good already for a $30 \times 30 \times 30$ k -point grid and that the results do not depend a lot on the smearing parameter for reasonable values in the mRy range.

For the phonon temperature T_p [entering the Bose distribution function in Eq. (4)], room temperature is chosen, $T_p = 300$ K, since the phonon heating is quite slow on a ps time scale.⁵⁹ Room temperature is considered as equilibrium temperature T_0 in Eq. (15), $T_0 = 300$ K, since most experiments are made at room temperature.

A. For ground-state exchange splitting

We calculate the demagnetization time τ_M according to Eq. (15) for fcc Ni and bcc Fe. It turns out that τ_M is about 16 fs for fcc Ni and about 22 fs for bcc Fe. Actually, the demagnetization time is less than the experimental demagnetization time (about 100 or 200 fs) and, therefore, spin-flip electron-phonon scattering is indeed fast enough to explain a demagnetization dynamics on the 100-fs time scale. This is astonishing because it was expected by many people that electron-phonon scattering processes can change observables in time only on a time scale which is larger than the oscillation time of one phonon period which is typically 1 ps.

With the demagnetization time at hand, it is possible to estimate the material-dependent proportionality factor p appearing in the Elliott-Yafet equation^{2,47,60}

$$\frac{1}{\tau_M} = pb^2 \frac{1}{\tau}, \quad (25)$$

where $b^2 = \langle \min(p_{jk}^\uparrow, p_{jk}^\downarrow) \rangle$ is the spin-mixing factor and $\langle \dots \rangle$ denotes the average over all states on the Fermi surface [$b^2 = 0.025$ for fcc Ni,⁴⁷ $b^2 = 0.024$ for bcc Fe (Ref. 47)]. τ is the Drude relaxation time which is about 2.4 fs for pure bcc Fe at 273 K.⁶¹ This yields a proportionality factor $p \approx 4.5$ which is perfectly in the range $1 < p < 10$ given by Beuneu and Monod for metals.⁶⁰ The spin-flip probability $a_{sf} = pb^2$ is about 0.11.

The demagnetization time does not say anything about the strength of demagnetization, it just says that any change of the magnetic moment occurs on such a short time scale. The information about the strength of demagnetization is contained in the demagnetization rate. The demagnetization rate dM/dt is calculated at time t_s for different electron temperatures $T_e(t_s)$ from 300 K up to 2000 K and the results are shown in Fig. 1 for the ground-state magnetic moment [Fig. 1(a) $0.64\mu_B$ for fcc Ni and Fig. 1(b) $2.2\mu_B$ for bcc Fe]. We consider the electron temperature $T_e(t_s)$ as an open parameter. As written above, electron temperatures up to 1000 K are reasonable and electron temperatures of 1500 or 2000 K are probably too large. The demagnetization rate $dM/dt(t_s)$ is almost zero for all electron temperatures in bcc Fe. Also, in fcc Ni $dM/dt(t_s)$ is almost zero for electron temperatures up to 1000 K, whereas

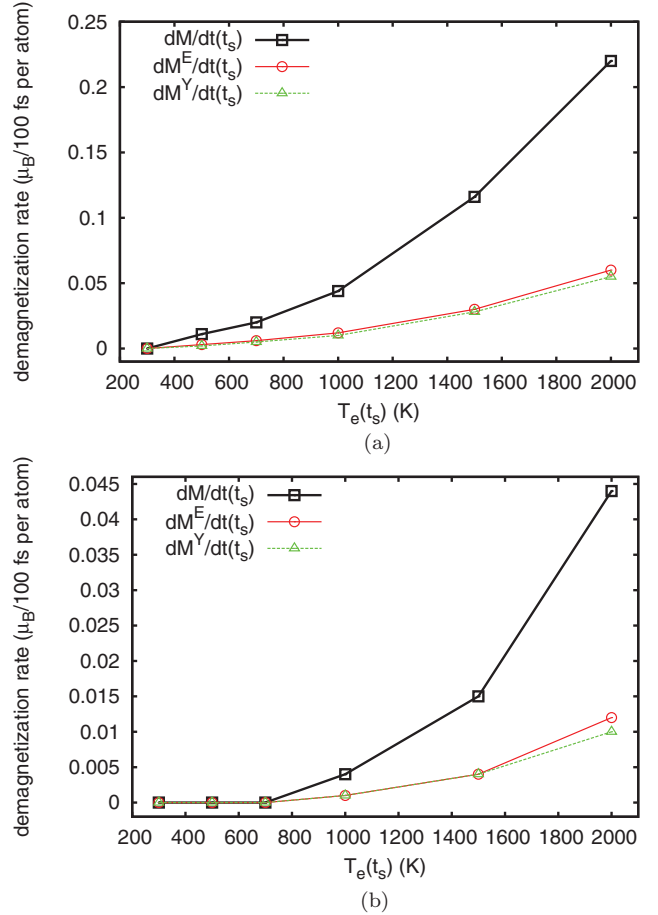


FIG. 1. (Color online) Calculated demagnetization rate $dM/dt(t_s)$ (black line, squares) at time t_s as a function of the electron temperature $T_e(t_s)$ for the ground-state exchange splitting according to the ground-state magnetic moment: (a) $0.64 \mu_B$ for fcc Ni. (b) $2.2 \mu_B$ for bcc Fe. The demagnetization rate is split into the Elliott part $dM^E/dt(t_s)$ (red line, circles) and the Yafet part $dM^Y/dt(t_s)$ (green line, triangles).

$dM/dt(t_s)$ equals about $0.12\mu_B/100$ fs for 1500 K and about $0.22\mu_B/100$ fs for 2000 K. Experimental demagnetization rates are about $0.2\mu_B/100$ fs for fcc Ni.⁴

We also split the results for the demagnetization rate $dM/dt(t_s)$ into an Elliott part $dM^E/dt(t_s)$ and a Yafet part $dM^Y/dt(t_s)$. The Elliott part considers only the modification of the effective potential due to the lattice distortion [first summand in Eq. (10)] and the Yafet part considers only the distortion-induced modification of the spin-orbit coupling [second summand in Eq. (10)]. The results are shown in Fig. 1. Whereas the sum of the Elliott part and the Yafet part of the matrix element yields the total matrix element, the sum of the Elliott part and the Yafet part of the demagnetization rate does not yield the total demagnetization rate $dM^E/dt(t_s) + dM^Y/dt(t_s) \neq dM/dt(t_s)$. We find that the Elliott part and the Yafet part make similar contributions to the total demagnetization rate which is in line with earlier publications⁶²⁻⁶⁴ on the spin relaxation of conduction electrons in Si, e.g., when switching off an external magnetic field.

B. For exchange splittings according to reduced magnetic moments

It was suggested in Ref. 20 that a calculation with a band structure that changes during the demagnetization process (“dynamic band structure”) could possibly enhance the demagnetization. The interaction of the electrons with photons and the electron-phonon scattering processes lead to a modification of the occupation numbers for single-electron states corresponding to the present band structure. One of the resulting effects is that the overlap of electronic wave functions changes, e.g., by excitations of $3d$ electrons to s or p states, and this may modify the exchange interactions. We will take into account only the effects on the exchange interactions resulting from a change of the total magnetic moment of the system. As discussed in point 1 of Sec. I, the magnetic moment directly after the excitation with the laser beam is more or less the magnetic moment of the ground state. Therefore, in our treatment the exchange interactions are not modified by the laser pulse itself. However, during the demagnetization the magnetic moment changes. Therefore, we also calculate the demagnetization rate $dM/dt(t_*)$ for band structures with reduced magnetic moment, i.e., reduced exchange splitting. We do this by a constrained density functional theory⁶⁵ by fixing the magnetic moment resulting from the solution of the Kohn-Sham equations by applying a Lagrangian field (which is determined self-consistently) to the value $M(t_*)$. t_* is the time at which the magnetic moment per atom is reduced to the value used for the calculation. We do not determine t_* but we consider the value $M(t_*)$ as a parameter, and we use the values $0.5\mu_B$, $0.4\mu_B$, and $0.3\mu_B$ per atom for fcc Ni and $1.6\mu_B$ and $1.1\mu_B$ per atom for bcc Fe. For Fermi’s golden rule, we then insert the electronic states which we get from the constrained band-structure calculation. The calculations are made for electron temperatures $T_e(t_*)$ from 300 K up to 1000 K, and it does not make sense to consider higher electron temperatures since the electron temperature has already cooled down at time t_* . The results are shown in Fig. 2. Indeed, the demagnetization rates in Fig. 2 are greater than the demagnetization rates in Fig. 1 for the same electron temperature. However, for bcc Fe and for all electron temperatures, the demagnetization rates $dM/dt(t_*)$ are much smaller than experimental demagnetization rates. The same holds for fcc Ni except for $T_e(t_*) = 1000$ K where the demagnetization rates are about $0.15\mu_B/100$ fs for a magnetic moment of $0.5\mu_B$, about $0.13\mu_B/100$ fs for a magnetic moment of $0.4\mu_B$, and about $0.09\mu_B/100$ fs for a magnetic moment of $0.3\mu_B$.

V. PHASE-SPACE ESTIMATION

In addition, we estimate the phase space for scattering (similar as in Ref. 20) which is linked to the maximum possible demagnetization for fcc Ni, bcc Fe, and fcc Co. Thereby, it is again assumed that thermalized electron distributions are mainly responsible for the demagnetization (see above).

The maximum possible demagnetization ΔM (more precisely, the maximum possible decrease of magnetic moment per atom) is achieved if all minority electrons do not flip their spins while all excited majority electrons ΔN^\uparrow flip their spin (excited with respect to the equilibrium situation at

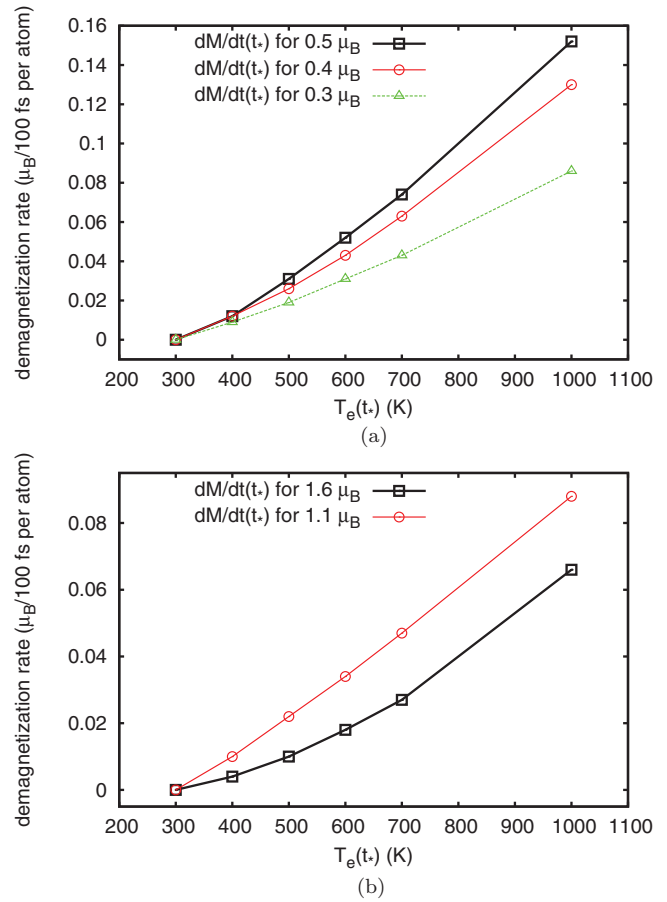


FIG. 2. (Color online) Calculated demagnetization rate $dM/dt(t_*)$ at time t_* as a function of the electron temperature $T_e(t_*)$ for different reduced exchange splittings according to reduced magnetic moments: (a) $0.5\mu_B$ (black line, squares), $0.4\mu_B$ (red line, circles) and $0.3\mu_B$ (green line, triangles) for fcc Ni. (b) $1.6\mu_B$ (black line, squares) and $1.1\mu_B$ (red line, circles) for bcc Fe. t_* is the time at which the magnetic moment per atom is reduced to the value used for the calculation.

$T_0 = 300$ K) and all excited minority holes $\Delta N^{h\downarrow}$ are filled by minority electrons which were majority electrons but flipped their spins. Since every spin-flip changes the magnetization by about $2\mu_B$, the maximum possible demagnetization is $\Delta M = 2\mu_B(\Delta N^\uparrow + \Delta N^{h\downarrow})$ per atom. The number of excited majority electrons ΔN^\uparrow and the number of excited minority holes $\Delta N^{h\downarrow}$ at time t_s is given by

$$\Delta N^\uparrow(t_s) = \int_{\varepsilon_i^\uparrow}^{+\infty} d\varepsilon Z^\uparrow(\varepsilon)[f_{t_s}(\varepsilon^\uparrow) - f_0(\varepsilon)],$$

$$\Delta N^{h\downarrow}(t_s) = \int_{-\infty}^{\varepsilon_i^\downarrow} d\varepsilon Z^\downarrow(\varepsilon)[f_0(\varepsilon) - f_{t_s}(\varepsilon^\downarrow)],$$
(26)

where ε_i^\uparrow is the intersection point of the functions $f_0(\varepsilon)$ and $f_{t_s}(\varepsilon^\uparrow)$ and ε_i^\downarrow is the intersection point of the functions $f_0(\varepsilon)$ and $f_{t_s}(\varepsilon^\downarrow)$. The calculation of ΔN^\uparrow and $\Delta N^{h\downarrow}$ at time t_* is analogous. This phase-space estimation is of course not restricted to electron-phonon scattering processes. It is in principle valid for any spin-flip scattering process involving small energies (such as phonon energies).

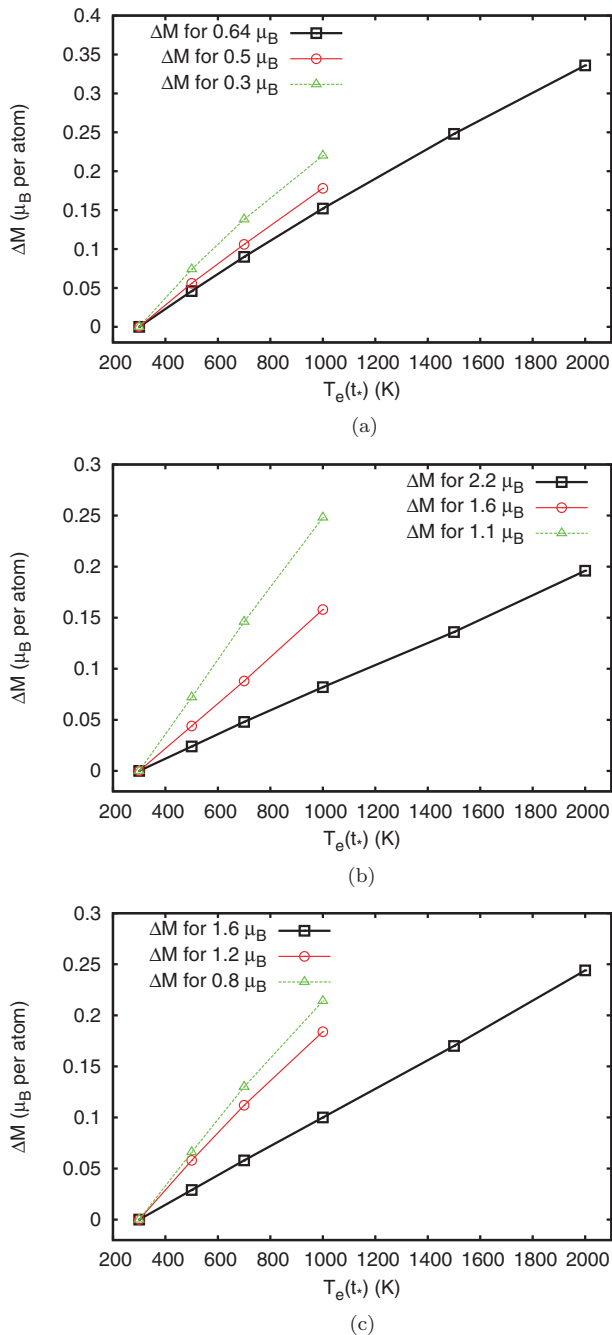


FIG. 3. (Color online) Calculated maximum possible demagnetization ΔM as function of the electron temperature $T_e(t_s)$ up to 2000 K for the ground-state exchange splitting according to the ground-state magnetic moment and up to 1000 K for reduced exchange splittings according to reduced magnetic moments. (a) fcc Ni: $0.64 \mu_B$ (black line, squares), $0.5 \mu_B$ (red line, circles) and $0.3 \mu_B$ (green line, triangles). (b) bcc Fe: $2.2 \mu_B$ (black line, squares), $1.6 \mu_B$ (red line, circles) and $1.1 \mu_B$ (green line, triangles). (c) fcc Co: $1.6 \mu_B$ (black line, squares), $1.2 \mu_B$ (red line, circles) and $0.8 \mu_B$ (green line, triangles).

Figure 3 shows the results for the phase-space estimation for electron temperatures up to 2000 K for the ground-state magnetic moment [Fig. 3(a), fcc Ni: $0.64 \mu_B$; Fig. 3(b), bcc Fe: $2.2 \mu_B$; Fig. 3(c), fcc Co: $1.6 \mu_B$] at time t_s and up to 1000 K for different reduced magnetic moments at time t_* . One can

see clearly that the maximum possible demagnetization $\Delta M = 2\mu_B(\Delta N^\uparrow + \Delta N^{h\downarrow})$ becomes larger if the magnetic moment is reduced. For the ground-state magnetic moment, the maximum possible demagnetization ΔM is much too small to explain an experimental demagnetization of 50% (about $0.32 \mu_B$ for fcc Ni, about $1.1 \mu_B$ for bcc Fe, and about $0.8 \mu_B$ for fcc Co) or even more, except for fcc Ni and an electron temperature of 2000 K. The maximum possible demagnetization ΔM is also quite small for bcc Fe and fcc Co with reduced magnetic moments and could not explain an almost total demagnetization which can be observed.⁴ This is not true for fcc Ni with reduced magnetic moments and an electron temperature of 1000 K.

To conclude, the phase space is too small for bcc Fe and fcc Co to explain an experimental demagnetization of 50% (about $1.1 \mu_B$ for bcc Fe and about $0.8 \mu_B$ for fcc Co) or even more (down to an almost total demagnetization), but it is not necessarily too small for fcc Ni. However, one has to keep in mind that most processes do not undergo spin flip and that ΔM is an absolute maximum. Therefore, it seems to be likely that the phase space is too small also for fcc Ni. Altogether, our result that the calculated demagnetization rate is smaller than the experimental rate (see Sec. IV) can be expected by these phase-space estimations for the case of bcc Fe and fcc Co, whereas for fcc Ni, explicit *ab initio* calculations are required.

VI. DISCUSSION AND CONCLUSIONS

In summary, the *ab initio* calculations of the demagnetization rates in Sec. IV could not reproduce experimental demagnetization rates for bcc Fe, neither for a band structure with ground-state magnetic moment nor for band structures with reduced magnetic moment. The same holds for fcc Ni except for very large electron temperatures ($T_e = 2000$ K for a band structure with ground-state magnetic moment, $T_e = 1000$ K for band structures with reduced magnetic moment), which are probably unrealistically large. We also come to similar conclusions in Sec. V: The maximum possible demagnetization is definitely too small for bcc Fe and fcc Co to explain an experimental demagnetization of about 50% (about $1.1 \mu_B$ for bcc Fe and of about $0.8 \mu_B$ for fcc Co) and even more (down to an almost total demagnetization), both for a band structure with ground-state magnetic moment and for band structures with reduced magnetic moment. This is not true for fcc Ni and large (probably unrealistic) electron temperatures.

Therefore, we conclude that the spin-flip electron-phonon scattering alone can not be the reason for the ultrafast demagnetization, i.e., we come to similar conclusions as in Refs. 19–22. However, we argued in Sec. I that the spin angular momentum has to go to the lattice in the end. The question arises as to how these two statements fit together. To answer this question, we discuss in the following a very recent publication.⁶⁶

It is shown in Ref. 66 that not only the longitudinal reduction, i.e., the length reduction of the magnetic moments must be considered (as we do in this paper), but also the transverse reduction, i.e., the disorder of the magnetic moments must be taken into account. It is demonstrated in model calculations that spin-flip electron-phonon scattering in a Stoner model can never reproduce ultrafast demagnetization, whereas the ultrafast demagnetization can be obtained in a model where

electron spin flips and atomic spin flips are respected. We want to give this model a microscopic interpretation in the following.

If a disorder of the magnetic moments is important for ultrafast demagnetization, one has to include magnons. We discuss now several processes where magnons are involved:

(1) As discussed in Sec. I, electron-magnon scattering alone can not change the spin angular momentum ($\langle \mathbf{S}_e \rangle$) without spin-orbit coupling. With spin-orbit coupling it is possible that angular momentum is transferred from $\langle \mathbf{S}_e \rangle$ to $\langle \mathbf{L}_e \rangle$ and thereafter $\langle \mathbf{L}_e \rangle$ could be very quickly quenched by the crystal field (faster than the temporal resolution of Refs. 24–26). In our opinion, crystal-field quenching is linked to electron-phonon scattering.

(2) Phonon-magnon scattering could also be a process where magnons are involved. For the relevance of phonon-magnon processes, see point 8 of Sec. I.

(3) In principle, also three-particle processes are possible, i.e., electron-phonon-magnon scattering processes, but they are definitely unlikely.

(4) It could also be that a combination of individual two-particle processes, i.e., spin-flip electron-phonon scattering and spin-flip electron-magnon scattering processes occur on a 100-fs time scale. Since angular momentum conservation is demanded for electron-magnon scattering without spin-orbit coupling (however, also with spin-orbit coupling angular momentum conservation is in a very good approximation fulfilled), only spin-down electrons can emit a magnon and flip their spin, $\downarrow \rightarrow \uparrow + \text{magnon}$, whereas only spin-up electrons can absorb a magnon and flip their spin, $\uparrow + \text{magnon} \rightarrow \downarrow$. Angular momentum conservation is not demanded for single electron-phonon scattering since linearly polarized phonons do not have a well-defined angular momentum (see Sec. I). Therefore, both spin-up and -down electrons can absorb or emit phonons. A combined spin-flip electron-phonon scattering and spin-flip electron-magnon scattering process where a magnon is emitted reads as

$$\begin{aligned} \uparrow + \text{phonon} &\rightarrow \downarrow \\ \downarrow &\rightarrow \uparrow + \text{magnon} \end{aligned} \quad (27)$$

or, alternatively,

$$\begin{aligned} \uparrow &\rightarrow \downarrow + \text{phonon}, \\ \downarrow &\rightarrow \uparrow + \text{magnon}. \end{aligned} \quad (28)$$

Thereby, the electron-phonon scattering is important for the transfer of angular momentum from the spin system to the lattice. The electron-magnon scattering is important for the disorder of the magnetic moments, which obviously leads to a demagnetization. Electron-phonon scattering processes are fast enough for a dynamics on a 100-fs time scale (see Sec. IV), and there are also hints that electron-magnon scattering processes are fast enough (see Refs. 3 and 67). It could be that the rate of electron-phonon scattering processes is as large as the rate of electron-magnon scattering processes. If the rates are different, then the slower process could determine the demagnetization dynamics. Investigations on this line are under way in our group (see also Ref. 68).

This list is certainly not complete. There are probably even more possible processes where magnons are involved. The fourth mechanism in the list (combined spin-flip electron-phonon and electron-magnon scattering processes) is certainly

the most likely mechanism of all and it is probably fast enough for a dynamics on the 100-fs time scale.

We want to note that it might also be that a combination of spin-flip electron-electron scattering and spin-flip electron-phonon scattering processes could be relevant for the demagnetization as already suggested in Refs. 27 and 28 for simple model calculations (see Sec. I). Krauss *et al.*²⁷ mention that the phase space for electron-electron scattering is much larger than the phase space for electron-phonon scattering since the phonon energy is very small (maximum: 40 meV). Electron-electron scattering is faster than electron-phonon scattering⁴ and, hence, many more electron-electron scattering processes take place which transfer the angular momentum from $\langle \mathbf{S}_e \rangle$ to $\langle \mathbf{L}_e \rangle$ in systems with spin-orbit coupling. Thereafter, the electron-phonon scattering processes could transfer the angular momentum to the lattice ($\langle \mathbf{L}_l \rangle$). The electron-phonon scattering could be the “bottleneck” which determines the speed of the demagnetization dynamics.

To conclude, the demagnetization time τ_M for fcc Ni and bcc Fe is even shorter than the experimental demagnetization time of about 100 fs, which shows that electron-phonon scattering is in principle fast enough for a dynamics on the 100-fs time scale. However, it was not possible to explain the strength of ultrafast demagnetization dM/dt for fcc Ni, bcc Fe, and fcc Co with spin-flip electron-phonon scattering alone, neither for a band structure with ground-state magnetic moment (which is in agreement with earlier publications^{19–22}) nor for band structures with reduced magnetic moments, i.e., reduced exchange splittings, except for fcc Ni and large (probably unrealistic) electron temperatures. We come to similar conclusions as in Ref. 66: In order to explain the ultrafast demagnetization, one should include magnons which lead to a disorder of the magnetic moments and lead obviously to a demagnetization. Since the angular momentum has to be transferred to the lattice (see Sec. I), also phonons must be included. We discuss that three-particle processes are unlikely and that phonon-magnon scattering is too slow. Finally, we suggest combinations of single two-scattering processes, namely, combined spin-flip electron-phonon and spin-flip electron-magnon scattering processes as a possible explanation of the ultrafast demagnetization dynamics. These combined processes are probably fast enough for a dynamics on the 100-fs time scale, can transfer the angular momentum to the lattice, and lead to a disorder of the magnetic moments. Furthermore, we admit that combined spin-flip electron-electron and spin-flip electron-phonon scattering processes might also be important since the phase space is considerably enlarged if electron-electron scattering is included. We suggest to test the results of the model calculations of Mueller *et al.*²⁸ on this mechanism by corresponding *ab initio* calculations.

Note added. Recently, Mueller *et al.*⁶⁹ published a paper on the effect of the dynamic exchange splitting during the ultrafast demagnetization.

ACKNOWLEDGMENTS

The authors thank M. Aeschlimann, K. Carva, B. Koopmans, P. M. Oppeneer, A. J. Schellekens, H. C. Schneider, and D. Steiauf for helpful discussions.

*faehnle@is.mpg.de

- ¹E. Beaurepaire, J. C. Merle, A. Daunois, and J. Y. Bigot, *Phys. Rev. Lett.* **76**, 4250 (1996).
- ²M. Föhnle and C. Illg, *J. Phys.: Condens. Matter* **23**, 493201 (2011).
- ³E. Carpena, E. Mancini, C. Dallera, M. Brenna, E. Puppini, and S. De Silvestri, *Phys. Rev. B* **78**, 174422 (2008).
- ⁴B. Koopmans, G. Malinowski, F. Dalla Longa, D. Steiauf, M. Föhnle, T. Roth, M. Cinchetti, and M. Aeschlimann, *Nat. Mater.* **9**, 259 (2010).
- ⁵M. Föhnle, M. Haag, and C. Illg, *J. Magn. Magn. Mater.* **347**, 45 (2013).
- ⁶B. Koopmans, M. van Kampen, and W. J. M. de Jonge, *J. Phys.: Condens. Matter* **15**, S723 (2003).
- ⁷F. Dalla Longa, J. T. Kohlhepp, W. J. M. de Jonge, and B. Koopmans, *Phys. Rev. B* **75**, 224431 (2007).
- ⁸G. P. Zhang and T. F. George, *Phys. Rev. B* **78**, 052407 (2008).
- ⁹G. P. Zhang and W. Hübner, *Phys. Rev. Lett.* **85**, 3025 (2000).
- ¹⁰J.-Y. Bigot, M. Vomir, and E. Beaurepaire, *Nat. Phys.* **5**, 515 (2009).
- ¹¹G. P. Zhang, W. Hübner, G. Lefkidis, Y. Bai, and T. F. George, *Nat. Phys.* **5**, 499 (2009).
- ¹²M. S. Si and G. P. Zhang, *J. Phys.: Condens. Matter* **22**, 076005 (2010).
- ¹³A. Eschenlohr, M. Battiato, P. Maldonado, N. Pontius, T. Kachel, K. Hollmack, R. Mitznerand, A. Föhlisch, P. M. Oppeneer, and C. Stamm, *Nat. Mater.* **12**, 332 (2013).
- ¹⁴E. Beaurepaire, G. M. Turner, S. M. Harrel, M. C. Beard, J.-Y. Bigot, and C. A. Schmuttenmaer, *Appl. Phys. Lett.* **84**, 3465 (2004).
- ¹⁵D. J. Hilton, R. D. Averitt, C. A. Meserole, G. L. Fisher, D. J. Funk, J. D. Thompson, and A. J. Taylor, *Opt. Lett.* **29**, 1805 (2004).
- ¹⁶E. E. Radescu and G. Vaman, *Phys. Rev. E* **65**, 046609 (2002).
- ¹⁷R. J. Elliott, *Phys. Rev.* **96**, 266 (1954).
- ¹⁸Y. Yafet, in *Solid State Physics*, Vol. 14, edited by F. Seitz and D. Turnbull (Academic, New York, 1963), p. 1.
- ¹⁹K. Carva, M. Battiato, and P. M. Oppeneer, *Phys. Rev. Lett.* **107**, 207201 (2011).
- ²⁰S. Essert and H. C. Schneider, *Phys. Rev. B* **84**, 224405 (2011).
- ²¹S. Essert and H. C. Schneider, *J. Appl. Phys.* **111**, 07C514 (2012).
- ²²K. Carva, M. Battiato, D. Legut, and P. M. Oppeneer, *Phys. Rev. B* **87**, 184425 (2013).
- ²³A. G. McLellan, *J. Phys. C: Solid State Phys.* **21**, 1177 (1988).
- ²⁴C. Stamm, T. Kachel, N. Pontius, R. Mitzner, T. Quast, K. Hollmack, S. Khan, C. Lupulescu, E. F. Aziz, M. Wietstruk, H. A. Dürr, and W. Eberhardt, *Nat. Mater.* **6**, 740 (2007).
- ²⁵C. Stamm, N. Pontius, T. Kachel, M. Wietstruk, and H. A. Dürr, *Phys. Rev. B* **81**, 104425 (2010).
- ²⁶C. Boeglin, E. Beaurepaire, V. Halté, V. López-Flores, C. Stamm, N. Pontius, H. A. Dürr, and J.-Y. Bigot, *Nature (London)* **465**, 458 (2010).
- ²⁷M. Krauss, T. Roth, S. Alebrand, D. Steil, M. Cinchetti, M. Aeschlimann, and H. C. Schneider, *Phys. Rev. B* **80**, 180407(R) (2009).
- ²⁸B. Y. Mueller, T. Roth, M. Cinchetti, M. Aeschlimann, and B. Rethfeld, *New J. Phys.* **13**, 123010 (2011).
- ²⁹B. Koopmans, in *Spin Dynamics in Confined Magnetic Structures II*, edited by B. Hillebrands and K. Ounadjela (Springer, Berlin, 2002), p. 253.
- ³⁰A. Einstein and W. J. de Haas, *Verhandl. Deuts. Phys. Ges.* **17**, 152 (1915).
- ³¹J. Stöhr and H. C. Siegmann, *From Fundamentals to Nanoscale Dynamics*, 1st ed. (Springer, Berlin, 2006).
- ³²W. Hübner and K. H. Bennemann, *Phys. Rev. B* **53**, 3422 (1996).
- ³³M. Wietstruk, A. Melnikov, C. Stamm, T. Kachel, N. Pontius, M. Sultan, C. Gahl, M. Weinelt, H. A. Dürr, and U. Bovensiepen, *Phys. Rev. Lett.* **106**, 127401 (2011).
- ³⁴M. Battiato, K. Carva, and P. M. Oppeneer, *Phys. Rev. Lett.* **105**, 027203 (2010).
- ³⁵M. Battiato, K. Carva, and P. M. Oppeneer, *Phys. Rev. B* **86**, 024404 (2012).
- ³⁶D. Rudolf, C. La-o-Vorakiat, M. Battiato, R. Adam, J. M. Shaw, E. Turgut, P. Maldonado, S. Mathias, P. Grychtol, H. T. Nembach, T. J. Silva, M. Aeschlimann, H. C. Kapteyn, M. M. Murnane, C. M. Schneider, and P. M. Oppeneer, *Nat. Commun.* **3**, 1037 (2012).
- ³⁷B. Pfau, S. Schaffert, L. Müller, C. Gutt, A. Al-Shemmary, F. Büttner, R. Delaunay, S. Düsterer, S. Flewett, R. Frömter, J. Geilhufe, E. Guehrs, C. M. Günther, R. Hawaldar, M. Hille, N. Jaouen, A. Kobs, K. Li, J. Mohanty, H. Redlin, W. F. Schlotter, D. Stickler, R. Treusch, B. Vodungbo, M. Kläui, H. P. Oepen, J. Lüning, G. Grübel, and S. Eisebitt, *Nat. Commun.* **3**, 1100 (2012).
- ³⁸B. Vodungbo, J. Gautier, G. Lambert, A. B. Sardinha, M. Lozano, S. Sebban, M. Ducouso, W. Boutu, K. Li, B. Tudu, M. Tortarolo, R. Hawaldar, R. Delaunay, V. López-Flores, J. Arabski, C. Boeglin, H. Merdji, P. Zeitoun, and J. Lüning, *Nat. Commun.* **3**, 999 (2012).
- ³⁹E. Turgut, C. La-o-vorakiat, J. M. Shaw, P. Grychtol, H. T. Nembach, D. Rudolf, R. Adam, M. Aeschlimann, C. M. Schneider, T. J. Silva, M. M. Murnane, H. C. Kapteyn, and S. Mathias, *Phys. Rev. Lett.* **110**, 197201 (2013).
- ⁴⁰A. J. Schellekens, W. Verhoeven, T. N. Vader, and B. Koopmans, *Appl. Phys. Lett.* **102**, 252408 (2013).
- ⁴¹L. Nordheim, *Ann. Phys. (NY)* **401**, 607 (1931).
- ⁴²W. H. Butler, *Physics of Transition Metals* (AIP, New York, 1980), p. 505.
- ⁴³C. Grimaldi and P. Fulde, *Phys. Rev. B* **55**, 15523 (1997).
- ⁴⁴A. K. Rajagopal and M. Mochena, *Phys. Rev. B* **57**, 11582 (1998).
- ⁴⁵J. Schilp, T. Kuhn, and G. Mahler, *Phys. Rev. B* **50**, 5435 (1994).
- ⁴⁶D. Steiauf, C. Illg, and M. Föhnle, *J. Magn. Magn. Mater.* **322**, L5 (2010).
- ⁴⁷D. Steiauf and M. Föhnle, *Phys. Rev. B* **79**, 140401(R) (2009).
- ⁴⁸D. Steiauf, C. Illg, and M. Föhnle, *J. Phys.: Conf. Ser.* **200**, 042024 (2010).
- ⁴⁹C. Ederer, Ph.D. thesis, Max Planck Institute for Metals Research and University of Stuttgart, 2003.
- ⁵⁰O. K. Andersen and O. Jepsen, *Phys. Rev. Lett.* **53**, 2571 (1984).
- ⁵¹J. P. Perdew and Y. Wang, *Phys. Rev. B* **33**, 8800 (1986).
- ⁵²J. P. Perdew and Y. Wang, *Phys. Rev. B* **45**, 13244 (1992).
- ⁵³C. Illg, B. Meyer, and M. Föhnle, *Phys. Rev. B* **86**, 174309 (2012).
- ⁵⁴P. Giannozzi, S. Baroni, N. Bonini, M. Calandra, R. Car, C. Cavazzoni, D. Ceresoli, G. L. Chiarotti, M. Cococcioni, I. Dabo, A. D. Corso, S. de Gironcoli, S. Fabris, G. Fratesi, R. Gebauer, U. Gerstmann, C. Gougoussis, A. Kokalj, M. Lazzeri, L. Martin-Samos, N. Marzari, F. Mauri, R. Mazzarello, S. Paolini, A. Pasquarello, L. Paulatto, C. Sbraccia, S. Scandolo, G. Sclauzero, A. P. Seitsonen, A. Smogunov, P. Umari, and R. M. Wentzcovitch, *J. Phys.: Condens. Matter* **21**, 395502 (2009).
- ⁵⁵D. Vanderbilt, *Phys. Rev. B* **41**, 7892 (1990).
- ⁵⁶J. P. Perdew, K. Burke, and M. Ernzerhof, *Phys. Rev. Lett.* **77**, 3865 (1996).
- ⁵⁷T. Roth, A. J. Schellekens, S. Alebrand, O. Schmitt, D. Steil, B. Koopmans, M. Cinchetti, and M. Aeschlimann, *Phys. Rev. X* **2**, 021006 (2012).

- ⁵⁸U. Atxitia, O. Chubykalo-Fesenko, J. Walowski, A. Mann, and M. Münzenberg, *Phys. Rev. B* **81**, 174401 (2010).
- ⁵⁹X. Wang, S. Nie, J. Li, R. Clinite, J. E. Clark, and J. Cao, *Phys. Rev. B* **81**, 220301 (2010).
- ⁶⁰F. Beuneu and P. Monod, *Phys. Rev. B* **18**, 2422 (1978).
- ⁶¹N. W. Ashcroft and N. D. Mermin, *Solid State Physics*, 1st ed. (Brooks Cole, London, 1976).
- ⁶²J. L. Cheng, M. W. Wu, and J. Fabian, *Phys. Rev. Lett.* **104**, 016601 (2010).
- ⁶³V. F. Gantmakher and Y. B. Levinson, in *Modern Problems in Condensed Matter Sciences*, Vol. 19, edited by V. M. Agranovich and A. A. Maradudin (North-Holland, Amsterdam, 1987).
- ⁶⁴J. Fabian and M. W. Wu, in *Handbook of Spin Transport and Magnetism*, Vol. 1, edited by E. Y. Tsybal and I. Žutić (Chapman and Hall/CRC Press, Boca Raton, 2012).
- ⁶⁵P. H. Dederichs, S. Blügel, R. Zeller, and H. Akai, *Phys. Rev. Lett.* **53**, 2512 (1984).
- ⁶⁶A. J. Schellekens and B. Koopmans, *Phys. Rev. Lett.* **110**, 217204 (2013).
- ⁶⁷A. B. Schmidt, M. Pickel, M. Donath, P. Buczek, A. Ernst, V. P. Zhukov, P. M. Echenique, L. M. Sandratskii, E. V. Chulkov, and M. Weinelt, *Phys. Rev. Lett.* **105**, 197401 (2010).
- ⁶⁸M. Haag, C. Illg, and M. Fähnle, *Phys. Rev. B* **87**, 214427 (2013).
- ⁶⁹B. Y. Mueller, A. Baral, S. Vollmar, M. Cinchetti, M. Aeschlimann, H. C. Schneider, and B. Rethfeld, *Phys. Rev. Lett.* **111**, 167204 (2013).